SACLANTCEN REPORT
serial no: SR-275

SACLANT UNDERSEA RESEARCH CENTRE REPORT

CHANNEL SENSITIVE PROCESSOR: SENSITIVITY AND OPTIMIZATION STUDY

G. Haralabus

October 1997

Report no. changed (Mar 2006): SR-275-UU

SACLANT Undersea Research Centre
Viale San Bartolomeo 400
19138 San Bartolomeo (SP), Italy

tel: +39-187-540.111
fax: +39-187-524.600

e-mail: library@saclantc.nato.int

NORTH ATLANTIC TREATY ORGANIZATION

SACLANTCEN SR-275

Channel Sensitive Processor: Sensitivity and Optimization Study

G. Haralabus

The content of this document pertains to work performed under Project 041-2 of the SACLANTCEN Programme of Work. The document has been approved for release by The Director, SACLANTCEN.

Jan L. Spoelstra
Director

intentionally blank page

Channel Sensitive Processor: Sensitivity and Optimization Study

G. Haralabus

Executive Summary: Matched filter methods are used extensively in Low Frequency Active Sonar (LFAS) systems for target detection purposes. The conventional matched filter has become the standard method of choice because it is a robust technique independent of the nature of the medium. However, it has been shown that in a shallow water environment, due to dense multipath conditions, the performance of this detection scheme is significantly degraded. The Channel-Sensitive Processor (CSP) was designed to improve the performance of the classical matched filter by incorporating information on propagation conditions.

The purpose of the present report is to present a sensitivity analysis of the CSP processor. As CSP utilizes *a priori* information about the acoustic channel, it is important to investigate the degree and extent to which the medium affects detection performance. The channel parameters which are examined are: the source (or target) range and depth, the sound velocity profile, the sediment-subbottom interface, and the sediment thickness. It has been found that the processor is more sensitive to the geometric than to the environmental parameters. When the correct parameter values are utilized, the CSP clearly outperforms the conventional matched filter. However, when there is a significant degree of mismatch between the actual parameter values and the ones assumed by the processor, the performance of the CSP is inferior to that of the matched filter. To overcome this problem, the CSP method has been utilized in conjunction with two global optimization algorithms based on the simulated annealing algorithm. These algorithms are able to search efficiently large configuration spaces which can not be explored exhaustively. It has been shown that, although optimization methods cause an increase of the processing time, they reduce the channel mismatch effect and improve considerably the detection performance of the CSP. The next step is the application of the CSP detector to real data. The project is expected to be completed by the end of 1997.

intentionally blank page

Channel Sensitive Processor: Sensitivity and Optimization Study

G. Haralabus

Abstract:

The detection performance of the Channel-Sensitive Processor (CSP) has been tested in dense multi-path conditions. It was demonstrated that, for a known propagation channel, the CSP outperforms the conventional matched filter technique. However, in an uncertain environment, the probability of detection decreases according to the degree of mismatch between the assumed and the actual channel characteristics. It was found that the processor is more sensitive to geometric parameters (source range and depth) than to environmental parameters (sound velocity profile, sediment-subbottom interface, sediment thickness). To overcome the performance degradation due to channel mismatch, the CSP method was utilized in conjunction with two global optimization algorithms: the classical simulated annealing (SA) and a multi-layer simulated annealing (MUSA) method. At the expense of processing time, it has been found that the optimization methods reduce the channel mismatch effect and improve considerably the detection performance of the CSP.

Keywords: Matched Filter (MF), Channel-Sensitive Processor (CSP), sensitivity study, global optimization, Simulated Annealing (SA), MUlti-layer Simulated Annealing (MUSA).

Contents

1 Introduction 1

2 Simulation configuration 3

3 Matched Filtering Techniques 5
3.1 Conventional Matched Filter (MF) 6
3.2 Incoherent Matched Filter (IMF) 6
3.3 Channel Sensitive (Matched Filter) Processor (CSP) 7
3.4 Discussion 7

4 Geometric and environmental parameters sensitivity 9
4.1 Source (or target) range and depth 9
4.2 Sediment-Subbottom interface 12
4.3 Sound Speed Profile 13
4.4 Sediment thickness 15
4.5 Discussion 15

5 Global optimization 24
5.1 Simulated Annealing (SA) 24
5.2 MUlti-layer Simulated Annealing (MUSA) 25
5.3 Discussion 26

6 Conclusions 30

References 31

1 Introduction

Active sonars make extensive use of matched filter methods for target detection. The conventional matched filter scheme is independent of the geoacoustic characteristics of the channel, and therein lies a good deal of its attraction. However, it has been demonstrated [1],[2],[3] that due to dense multipath conditions the matched filter output can be so distorted that the induced detection results have a low degree of confidence. One way to overcome this problem is by incorporating existing information about propagation conditions in the detection algorithm. A detection algorithm based on this idea is the Channel Sensitive Processor (CSP) [4]. The detection performance of the CSP is not only improved compared to the traditional matched filter, but also this performance enhancement is valid in both a white noise and a reverberation limited environment. However, it was observed that when the assumed geometric and geoacoustic parameters of the medium are different from the actual parameters, the performance of the CSP is significantly degraded.

The purpose of this report is to examine the sensitivity of the CSP processor to environmental conditions, and propose methods to overcome this problem. Parameters which control the sound propagation in a waveguide, such as sound speed profile (SSP), sediment-subbottom interface, sediment thickness, source range and source depth, have been considered. The influence each parameter has on the CSP is examined separately and in conjunction with the rest of the parameters. Also, as the precise knowledge of the propagation channel is an unrealistic assumption, it is important to propose processing schemes which compensate for the environmental mismatch. Usually, this is succeeded by using global search methods, i.e., time efficient algorithms which search the parameter landscape to locate the parameter set which characterizes best the propagation environment. Two methods of this kind that have been successfully applied to underwater acoustics are the simulated annealing (SA) and the genetic algorithms. For programming convenience with the simulation set up used here, the former scheme is employed. SA is coupled with the CSP to compensate for the lack of *a priori* knowledge of the medium.

This report is organized in the following way: Section 2 describes the configuration of the experiment. Section 3 gives an overview of the CSP and its comparison with an incoherent matched filter (IMF) technique, and the classical matched filter (MF) method. Section 4 analyzes the sensitivity of the CSP to environmental mismatch. Section 5 is concerned with the utilization of global search in matched filtering and

focuses on optimizing the performance of the CSP. Finally, conclusions and ideas for improving upon the proposed methods are presented.

2 Simulation configuration

The SNAP [5] program has been used to create a range independent acoustic channel, subdivided into a 100 m water column, a sediment layer and a semi-infinite subbottom. As a result of the downward refracted, Mediterranean summer SSP's which are used here, dense multipath propagation conditions are induced. The waveguide is assumed to be homogeneous in azimuth. The source is placed at 70 m depth and 1300 m from the receiver which is situated at 65 m depth (see Fig. 1). The transmitted signal is an LFM pulse centered at 575 Hz with a 200 Hz bandwith.

The sensitivity study for the environmental parameters comprises 7 variations of a baseline SSP, 3 different sediment-subbottom interfaces (silt-sand, sand-gravel, and gravel-chalk), and 3 different sediment thickness (1 m, 3 m, and 10 m). The location search grid is extended from 1200 m to 1420 m in range (12 discrete points spaced 20 m apart), and from 50 m to 80 m in depth (7 points spaced 5 m apart). Therefore, the total number of scenarios simulated and stored (using MATLAB software program [6]) is 5292.

Every case represents a new realization of the propagation channel and is characterized by its own transfer function. One of these cases is chosen randomly to represent the real propagation channel. The "real data" pressure field is compared with the pressure fields generated using the remaining 5291 scenarios. Then, the detection performance of each processor is assessed.

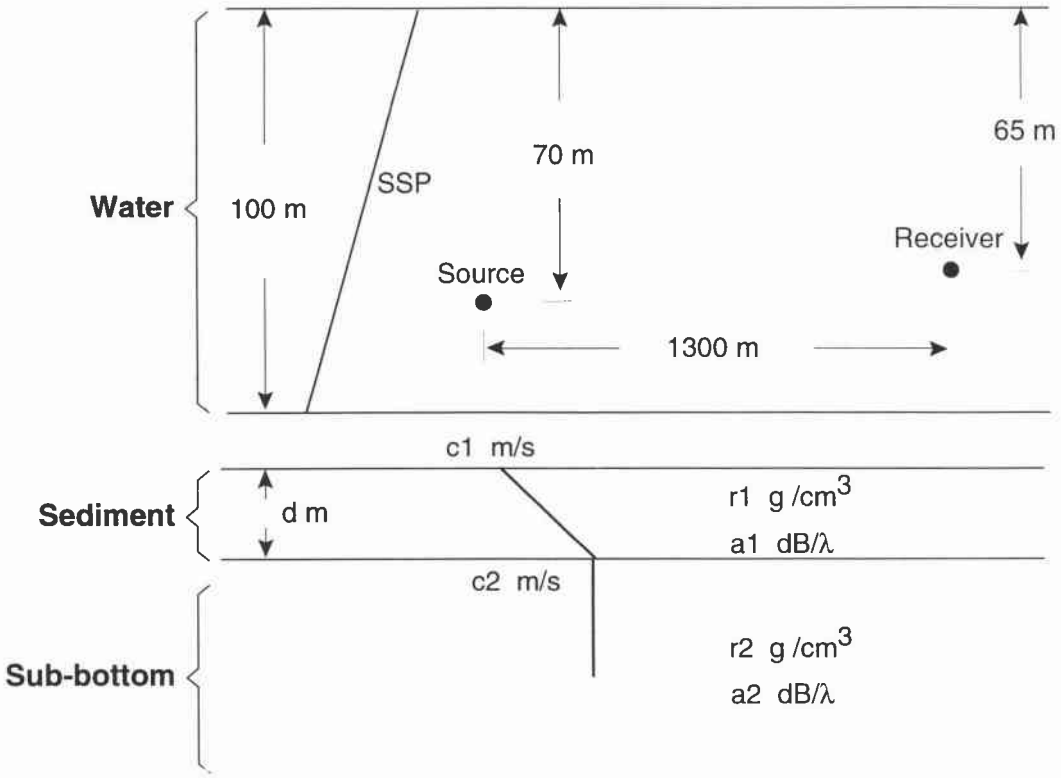

Figure 1 *Simulation geometry (not to scale).*

3

Matched Filtering Techniques

This section describes the matched filter techniques applied in this study. The matched filter is a linear time-invariant filter designed to maximize the peak pulse signal in the presence of noise [7], [8] i.e.,

$$\Lambda = \max \frac{|f_o(t)|^2}{\overline{n_o^2(t)}} = \frac{|f_o(t_m)|^2}{\hat{n}} \tag{1}$$

where $t = t_m$ is the optimum observation time, and $\hat{n} = \overline{n_o^2(t)}$ denotes the mean-squared value of the noise (independent of t).

For an LFM transmitted signal [9] with spectrum $S(\omega)$, and additive white noise with spectrum

$$S_n(\omega) = \frac{N_o}{2} \tag{2}$$

the general expression for the matched filter output can be written as [4], [7]

$$\Lambda = \frac{|f_o(t_m)|^2}{\hat{n}} = \frac{1}{N_o \pi} \frac{\left| \int_{-\infty}^{+\infty} G(\omega) S(\omega) H(\omega) \exp(-j\omega t_m) d\omega \right|^2}{\int_{-\infty}^{+\infty} |H(\omega)|^2 d\omega} \tag{3}$$

where $G(\omega)$ is the transfer function of the channel, and $H(\omega)$ is a general expression for the transfer function of the desired matched filter.

3.1 Conventional Matched Filter (MF)

For the conventional matched filter algorithm, the filter transfer function is independent of the propagation channel and can be written:

$$H(\omega) = S^*(\omega)\exp(j\omega t_m) \tag{4}$$

Combining Eq. (3) and Eq. (4), the expression for the MF output becomes:

$$\Lambda_{mf} = \frac{1}{\pi N_o}\frac{\left|\int_{-\infty}^{+\infty} G(\omega)|S(\omega)|^2 d\omega\right|^2}{\int_{-\infty}^{+\infty}|S(\omega)|^2 d\omega} \tag{5}$$

3.2 Incoherent Matched Filter (IMF)

Incoherent matched filter methods (IMF) differ from the classical MF in that they are based on more than one observation of the received signal. The output of the IMF filter, instead of being the maximum correlation value, is an incoherent summation of a number of maxima points of the correlation sequence of the transmitted and the received signal. In order to select the maximum and the secondary maxima values the user should specify criteria such as the noise level threshold, and estimate the time-spreading of the transmitted signal to avoid combination of peaks from different returns. Other variations of the IMF scheme instead of summing individual peaks are intergating the matched filter ouput over high-correlation time windows. Because in the window integration method there is a significant trade-off between signal peaks and unwanted noise spikes, the present study uses the former, incoherent summation technique. In general, IMF is an intuitively meaningful and practical scheme without particular theoretical treatment.

The transfer function of the IMF filter can be written in the following form

$$H(\omega) = S^*(\omega)[\exp(j\omega t_1) + \cdots \exp(j\omega t_m) + \cdots \exp(j\omega t_N)] \tag{6}$$

$$\Lambda_{imf} = \frac{1}{\pi N_o} \frac{\left| \int_{-\infty}^{+\infty} G(\omega)|S(\omega)|^2 \left[\exp(-j\omega t_{m_1}) \cdots + 1 + \cdots + \exp(-j\omega t_{m_N})\right] d\omega \right|^2}{\int_{-\infty}^{+\infty} |S(\omega)|^2 d\omega} \tag{7}$$

where $t_{m_1} = t_m - t_1$, $t_{m_N} = t_N - t_1$.

3.3 Channel Sensitive (Matched Filter) Processor (CSP)

The CSP is a channel sensitive type of matched filter technique. The main characteristic of this filter is that the transfer function of the CSP includes the transfer function of the medium, i.e.,

$$H(\omega) = kG^*(\omega)S^*(\omega)\exp(j\omega t_m) \tag{8}$$

and the CSP output can be expressed as

$$\Lambda_{csp} = \frac{1}{\pi N_0} \int_{-\infty}^{+\infty} |G(\omega)|^2 |S(\omega)|^2 d\omega \tag{9}$$

For more details about the derivation of these formulas, refer to [4].

3.4 Discussion

The detection performance of a receiving system is calculated by determining the probability of detection and the probability of false alarm for a given signal to noise ratio (SNR). This detection performance is presented graphically by plotting Receiver Operation Characteristics (ROC) curves. In these curves, the probability of detection is plotted *versus* the probability of false alarm for different thresholds [10]. Figure 2 shows the ROC curves for the MF, IMF (four peaks considered), and CSP cases for SNR=-23 dB. All cases have been created under precisely known propagation conditions (matched case). Overall, the CSP defines the upper limit of detection performance in matched filtering. IMF and MF have similar performance, with IMF

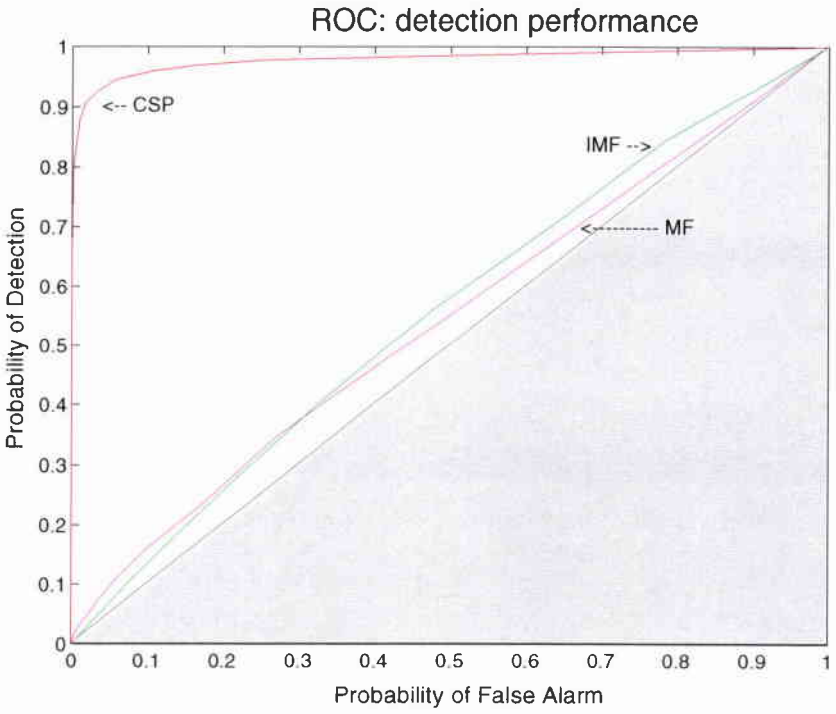

Figure 2 *ROC plots of the three filters,i.e., MF, IMF, and CSP. In all cases the propagation channel parameters are known (matched cases).*

having higher propability of detection than MF for increasing probability of false alarm. In the next 6 sections, the detection performance of the CSP processor in an uncertain environment (mismatched case) will be compared with the performance of the classical MF (lower bound) and with the performance of the CSP for the matched case (upper bound).

In deriving the above formulae it has been assumed that the main noise source is ambient noise. However, provided that the reverberation spectrum retains a high degree of correlation with the power spectrum of the transmitted signal [11], the same formulae are valid for a reverberation limited environment [4]. This is a particularly interesting result as when processing signals corrupted with reverberation, the SNR cannot be improved by increasing the power of the transmitted signal. The CSP method can however improve the SNR by combining coherently acoustic sound fields propagated along different paths.

4

Geometric and environmental parameters sensitivity

As shown in Eq. (8), the CSP method uses the transfer function of the channel to increase the correlation between the transmitted and the received pressure field. Consequently, the discrepancies between the modelled and the actual transfer function have a direct impact on the detection result. This section focuses on evaluating the performance degradation of the CSP algorithm due to mismatch between the "real" and the synthetic propagation channel. The uncertain parameters considered here are: source (or target) range and depth (geometric parameters), SSP, sediment-subbottom interface, and thickness of the sediment layer (environmental parameters). The sensitivity of the CSP processor to channel parameter mismatch has been examined separately for each parameter. ROC plots have been created for each case and are compared to the ones from the MF and CSP (matched) cases.

4.1 Source (or target) range and depth

Knowledge of the experimental geometry implies source or target localization in a passive or active sense respectively. The sensitivity of the detection algorithm to the source (or target) range and depth depends on the algorithm itself, the environmental conditions, and the deployed systems (vertical or towed arrays, buoys, etc.). Detection performance in shallow water is affected mainly by the multipath propagation conditions and the interaction of the acoustic field with the channel boundaries. Acoustic rays arriving at the receiver from different paths create such a complicated interference pattern that small changes in range or depth significantly alter the overall received pressure field [12]. The ambiguity surface shown in Fig. 3 compares the performance of the conventional MF with the CSP result, and serves as an initial indication on how sensitive the CSP technique is to uncertainty of the source (or target) coordinates. Figures 4 and 5 show the ROC curves for the range and depth mismatched cases respectively. In both cases the detection performance of CSP is significantly degraded. This can be attributed mainly to the complicated multipath pattern of the propagated sound field which changes significantly as a function of range and depth; yet another demonstration that target detection and localization is a very complex task in shallow water.

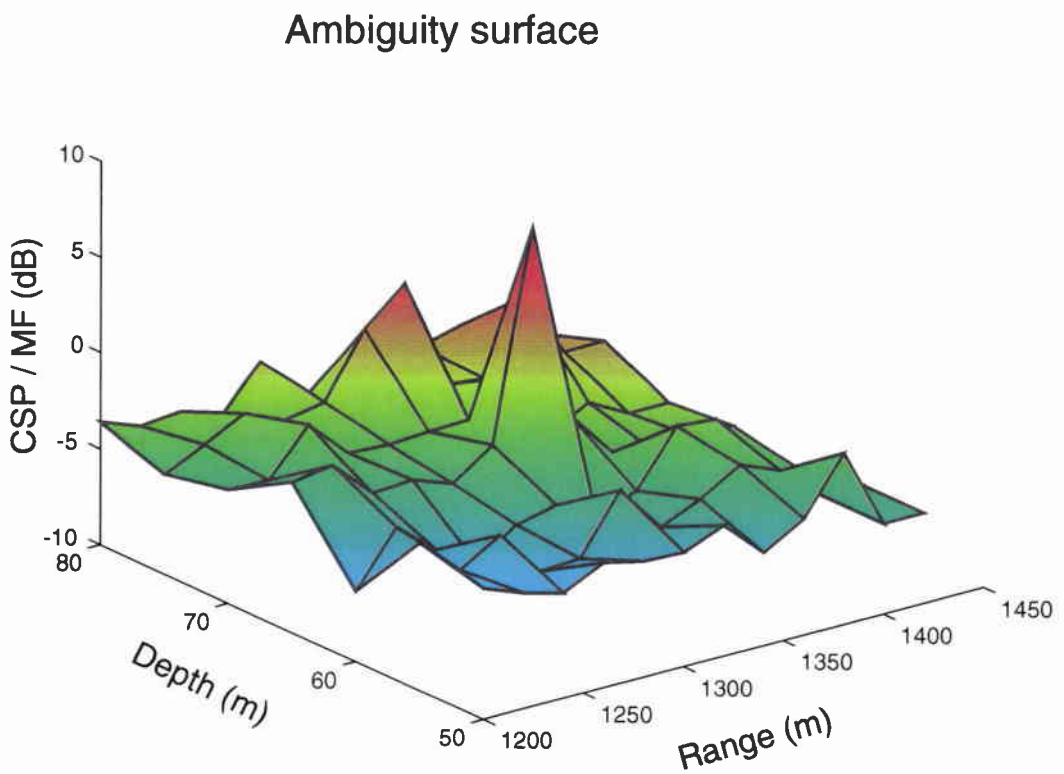

Figure 3 *Ambiguity surface of the ratio of the CSP and the MF detection output. The maximum CSP-to-MF gain is approximately 8 dB while the max CSP-to-MF mismatch reduction is approximately -5 dB.*

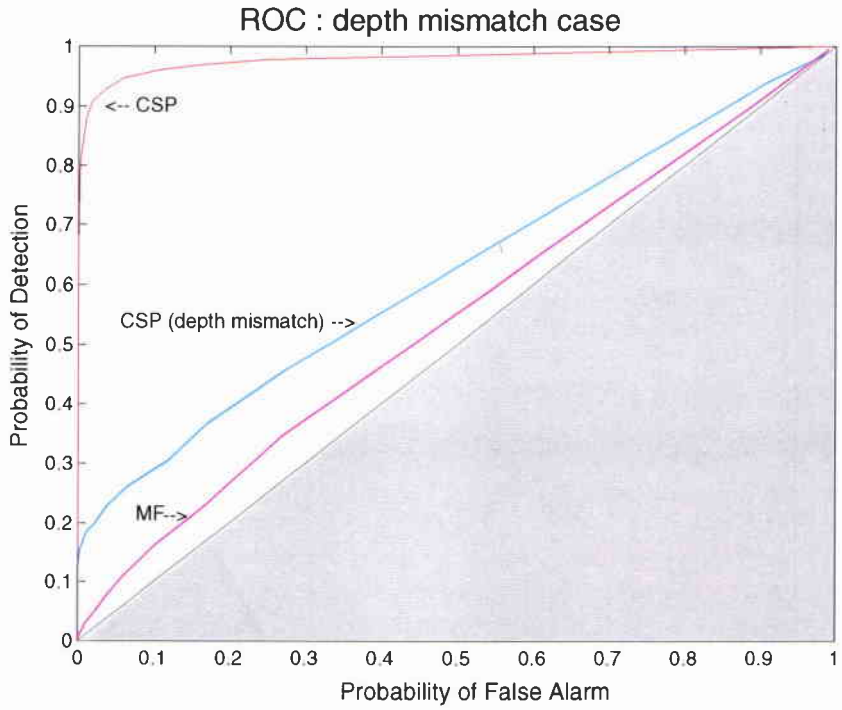

Figure 4 *ROC plots for performance comparison between the matched case CSP, the depth mismatched case CSP, and the MF processor.*

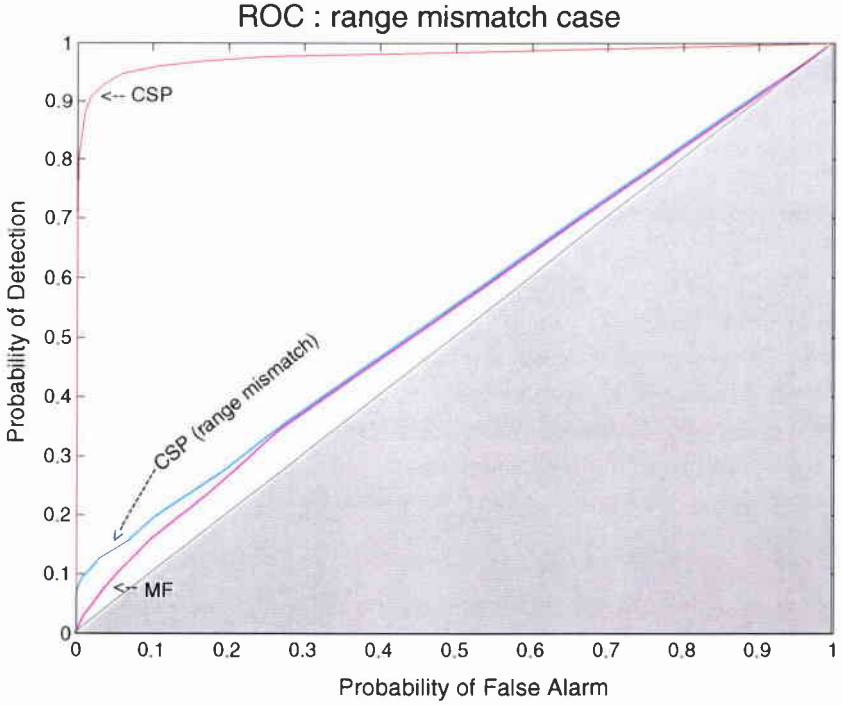

Figure 5 *ROC plots for performance comparison between the matched case CSP, the range mismatched case CSP, and the MF processor.*

4.2 Sediment-Subbottom interface

In a shallow water environment, sound interaction with the seafloor has a strong influence on the transmitted pressure field. Therefore, in a sensitivity study the bottom structure becomes important.

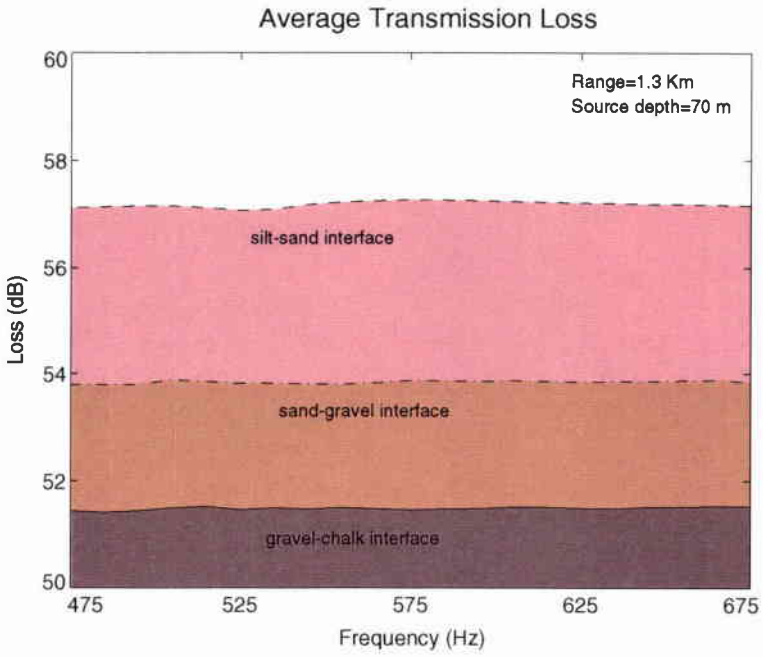

Figure 6 *Average water column transmission loss vs frequency for all three sediment-subbottom interfaces.*

Conventionally, the seafloor is best described using a geoacoustic model which provides information about the water mass above the sediment, depth-dependent values of both water and bottom density, and the speed and the attenuation of both compressional and shear waves. In the present study, three types of sediment-subbottom interfaces with different properties have been considered: a) silt-sand, b) sand-gravel, and c) gravel-chalk. The first two are typical continental terrace interfaces generated from terrigenous sources. The third is a rock-type acoustic basement which covers ocean plateau, and seamounts [13].

The sediment in cases a) and b) is considered to be a "soft layer" and is frequently modelled as fluid (supporting only compressional waves). On the contrary, the sediment in c) posses enough rigidity to be modelled as elastic (supporting both compressional and shear waves) [14]. The shear wave affect (a low-frequency mechanismwhich dissipates acoustic energy from the water column through sound interaction with the bottom) increases monotonically with sediment thickness and

	comp. wave speed	*comp. wave attenuation*	*density*
Silt	1575 (m/sec)	1.0 (dB/λ)	1.7 (kg/m^3)
Sand	1650 (m/sec)	0.8 (dB/λ)	1.9 (kg/m^3)
Gravel	1800 (m/sec)	0.6 (dB/λ)	2.0 (kg/m^3)
Chalk	2400 (m/sec)	0.2 (dB/λ)	2.2 (kg/m^3)

Table 1 *Geoacoustical parameters used for modelling silt, sand, gravel, and chalk interfaces.*

decreasing frequency [15]. As here the frequencies of interest are greater than 0.5 kHz and the sediment thickness is always equal or less than 10 m, the shear speed can be disregarded. Table 1 summarizes the geoacoustic properties of the three bottom types [14]. In each, the maximum sediment thickness is 10 m which corresponds approximately to three wavelenghts. As shown in Fig. 6, for every sediment-subbottom interface examined the average water column transmission loss is constant over the frequency band of the transmitted LFM signal. Therefore, for demonstration purposes, the propagation contour loss plots shown correspond only to the central frequency of 575 Hz.

Figure 7 shows twelve modes for each case. Although the first six modes behave similarly for all surfaces, the high order modes are able to penetrate only the "soft" sediments.

Figure 8 shows propagation loss contour plots for all three cases. The "soft", sound absorbing silt-sand terrain has the highest propagation loss values. On the contrary, the rigid, sound reflecting gravel-chalk surface has the lowest values.

The ROC curves for the sediment-subbottom mismatched case are shown in Fig. 9. The detection performance is degraded relative to the matched case but is superior to that of the classical MF.

4.3 Sound Speed Profile

There are invariably discrepancies between measured and actual SSP's. Depending on whether the processing method relies on precise or average measurements of the SSP, such inaccuracies could significantly affect the experimental outcome.

The CSP method used in the present analysis is based on the waveguide multipath induced by the channel geometry and the SSP. Therefore, accurate measurements of SSP are of foremost importance in utilizing the CSP; for this reason sound velocity mismatch is investigated.

The permutations of the SSP are created using a real profile modified by random variations which obey a Gaussian spectrum. In particular, the generating function of the SSP is given by

$$p(x_n) = [p_0(x_n) + f(x_n)] \exp(-cx_n^2) \tag{10}$$

where $p_0(x_n)$ is the baseline profile, $\exp(-cx_n^2)$ is an exponential term which controls the amplitude of the perturbation. Due to diurnal temperature changes and water mixing at the sea surface, the deviation of the SSP from the baseline model is greater at the surface layer than at the lower layers. The term $\exp(-cx_n^2)$, with c constant, guarantees that the amplitude of the SSP perturbation decreases monotonically with depth. The perturbation term is defined by the formula:

$$f(x_n) = \frac{1}{L} \sum_{j=-N/2}^{N/2-1} F(K_j) \exp(iK_j x_n) \tag{11}$$

where $j \geq 0$,

$$F(K_j) = [2\pi L W(K_j)]^{1/2} \begin{cases} [N(0,1) + iN(0,1)]/\sqrt{2} & j \neq 0, N/2 \\ N(0,1) & j = 0, N/2 \end{cases} \tag{12}$$

where the water depth is $L = N\Delta x$, N the total number of points, Δx is the spacing between points, $F(K_j) = F(K_{-j})^*$ for $j \leq 0$, $K_j = 2\pi j/L$, $N(0,1)$ each time is used indicates a zero mean, unit variance Gaussian distributed random number, and $W(K)$ is the spectrum of the distribution

$$W(K) = (lh^2/2\sqrt{\pi}) \exp(-K^2 l^2/4) \tag{13}$$

where h denotes the root-mean-squared deviation and l the profile's correlation length.

This method of creating random perturbation of the SSP is based on a random surface generation technique described in [16]. Figure 11 shows the seven profiles used in this study. Figure 10 displays propagation loss contour plots for three SSP's.

In spite the fact that in these three cases the propagation loss values are of the same order of magnitude, the energy distribution changes. This change is reflected in the CSP output as it is shown from the ROC plots in Fig. 12.

4.4 Sediment thickness

In modelling a layered bottom, another parameter that should be taken into account is the thickness of each layer. The effect of this parameter is inversely proportional to the frequency of the incident waves, as the sound interaction with the seafloor decreases with increasing frequency [17]. At high frequencies, the effective penetration depth is in the upper few metres or tens of metres [15], [13]. In the present study, the bottom is modelled as a sediment layer overlying a semi-infinite subbottom. For the sediment thickness three values are examined, i.e. 1 m, 3 m, and 10 m, which correspond to approximately 0.3, 1, and 3 wavelengths. Figure 13 shows propagation loss contour plots for the silt-sand interface for all cases. As expected, absorbtion of acoustic energy increases with the sediment thickness. Figure 14 demonstrates the ROC plots. It can be seen that sediment thickness uncertainty has little effect on the detection performance by comparison with other environmental parameters.

4.5 Discussion

As expected, the CSP detector is very sensitive to propagation conditions uncertainty. For partial mismatched cases (one uncertain parameter only) it has been shown that in a dense multipath channel, the detection performance is degraded more for geometric than environmental parameter mismatch. As shown in Fig. 15, for total mismatched case (all channel parameters are uncertain) the CSP detection performance is degraded below that of the classical MF method.

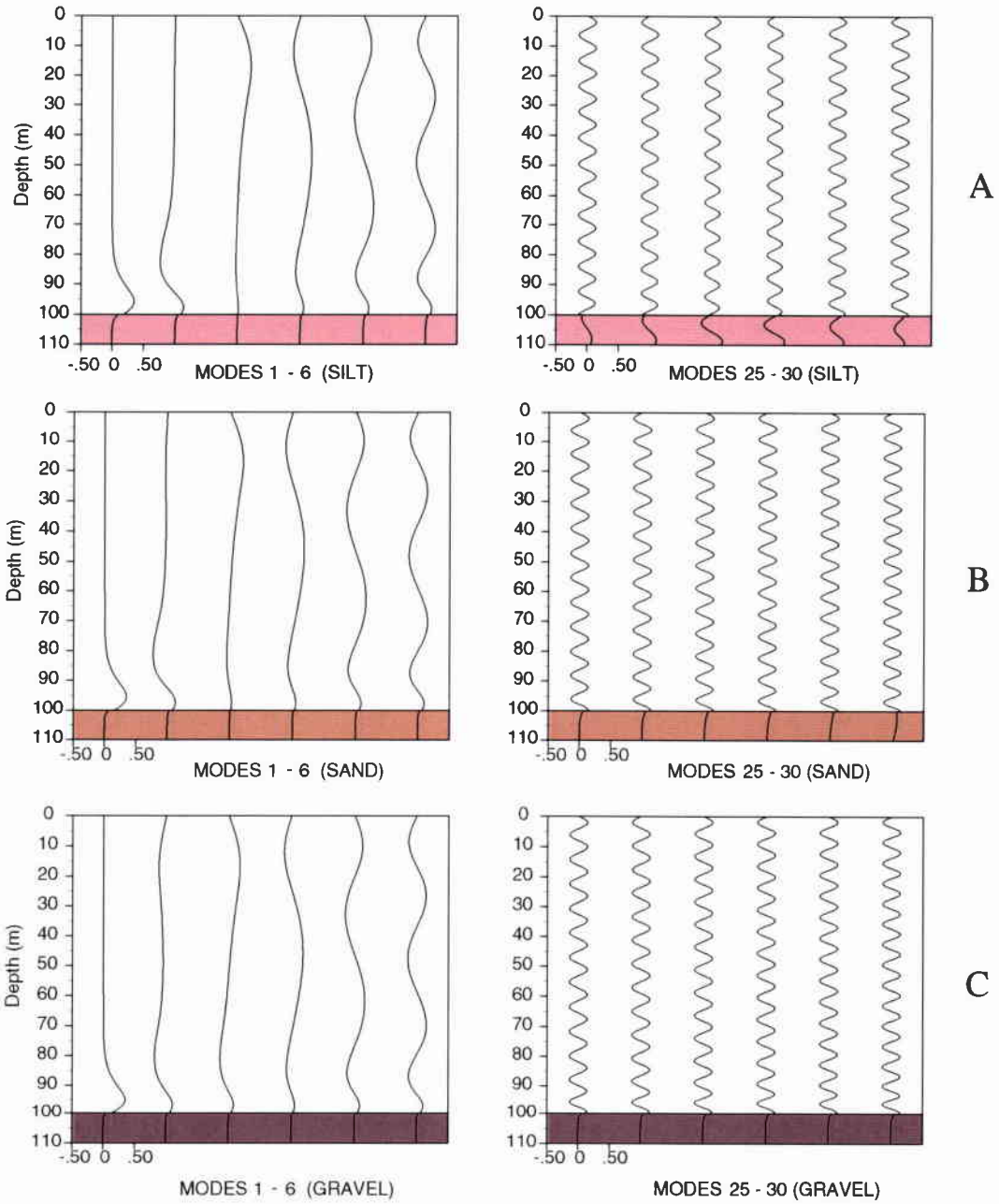

Figure 7 *Modes (1-6, 25-30) for the three sediment types considered here: A) silt, B) sand, C) gravel.*

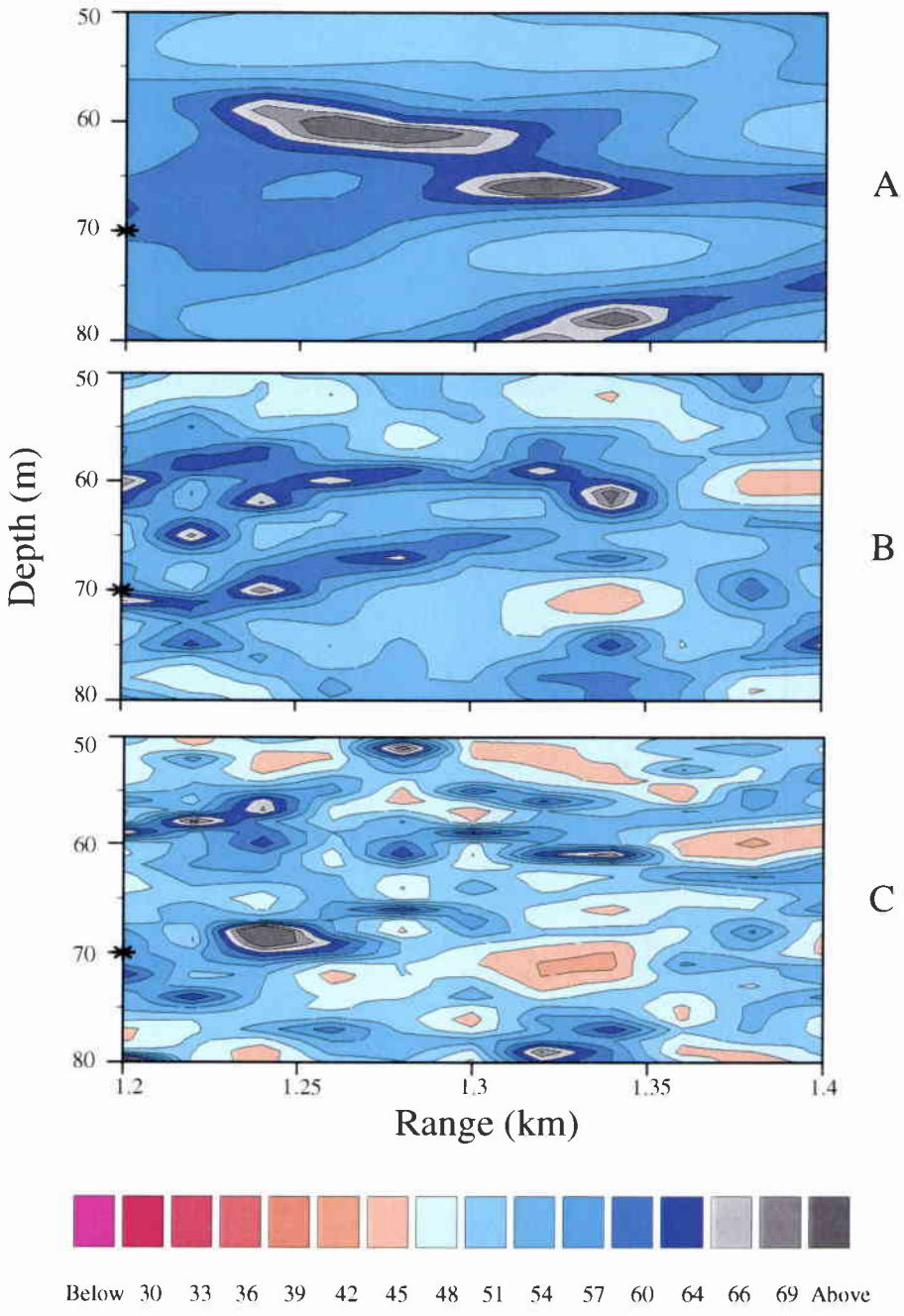

Figure 8 *Transmission loss plots for three types of subbottom-sediment interface: A) silt-sand, B)sand-gravel, and C) gravel-chalk. The source depth is 70 m, and the frequency is 575 Hz.*

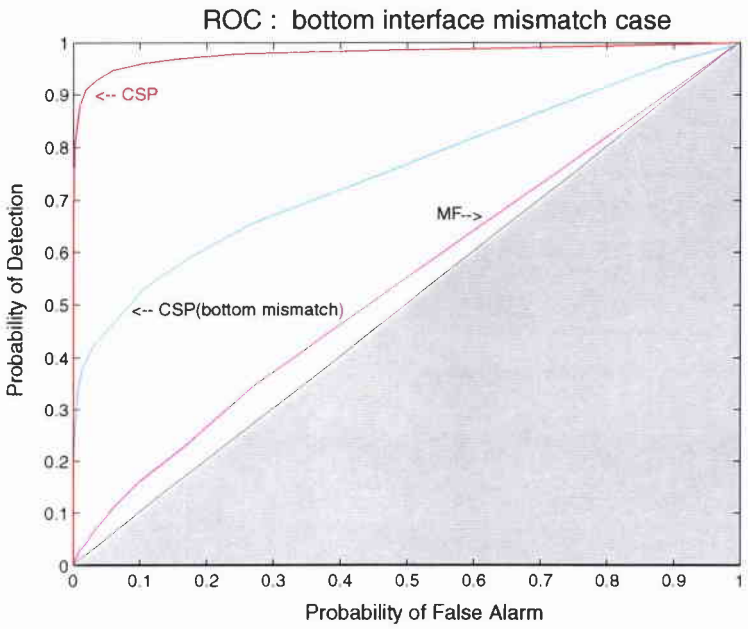

Figure 9 *ROC plots for performance comparison between the matched case CSP, the bottom mismatched case CSP, and the MF processor.*

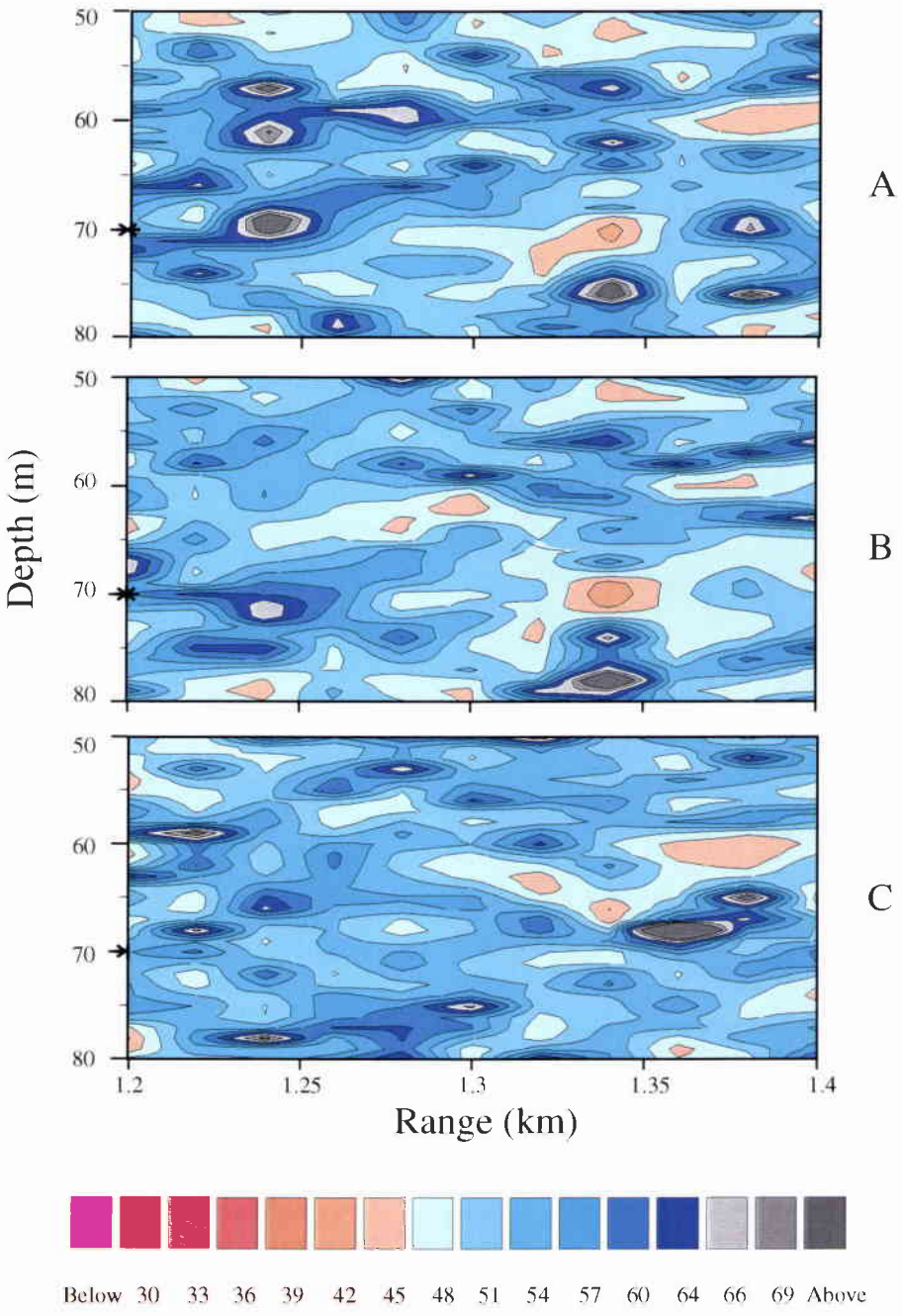

Figure 10 *Transmission loss plots for three sound velocity profiles. The sand-gravel interface has been used with sediment thickness 1 m. The source depth is 70 m, and the frequency is 575 Hz.*

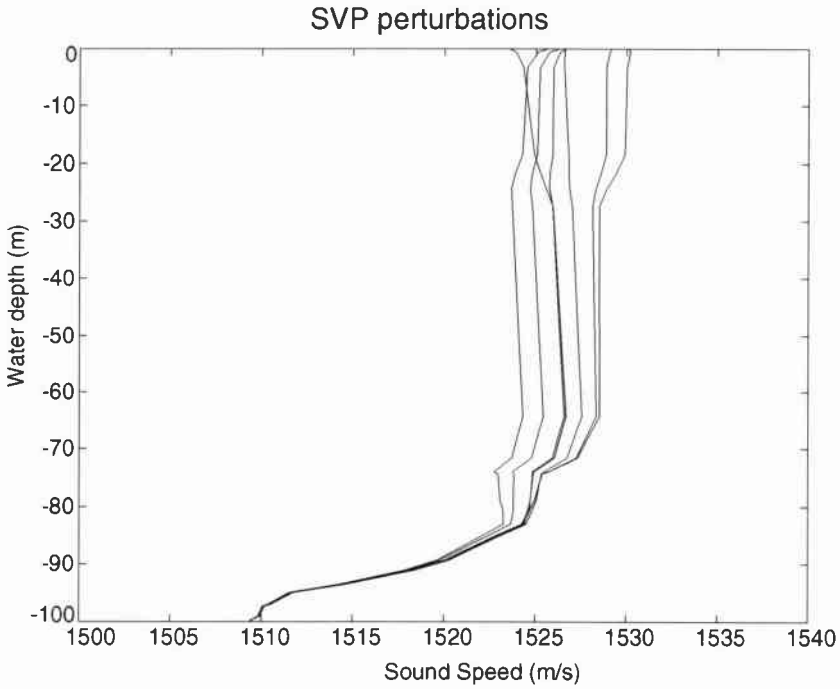

Figure 11 *Perturbations of the sound speed profiles.*

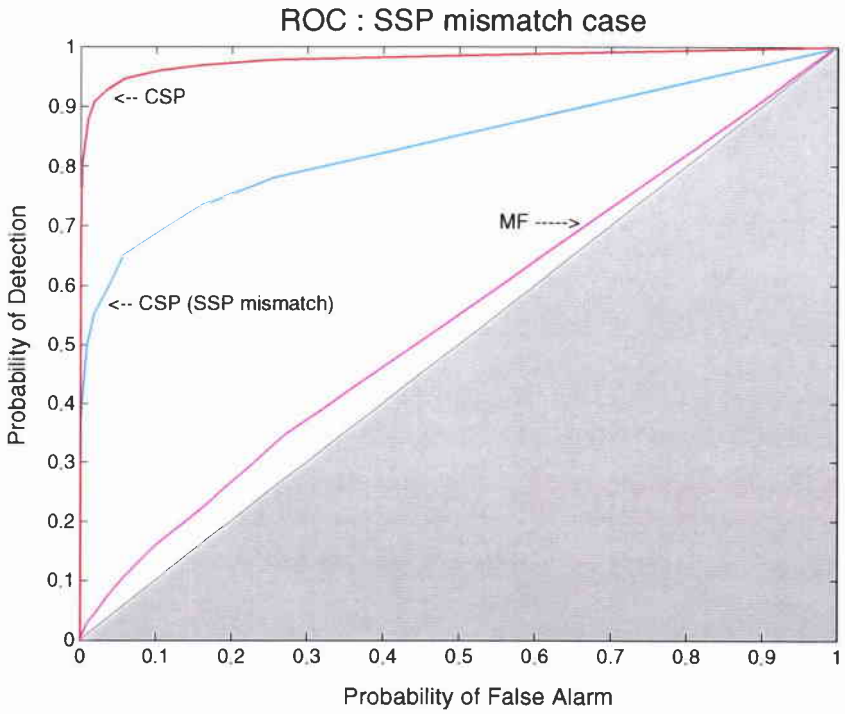

Figure 12 *ROC plots for performance comparison between the matched case CSP, the SSP mismatched case CSP, and the MF processor.*

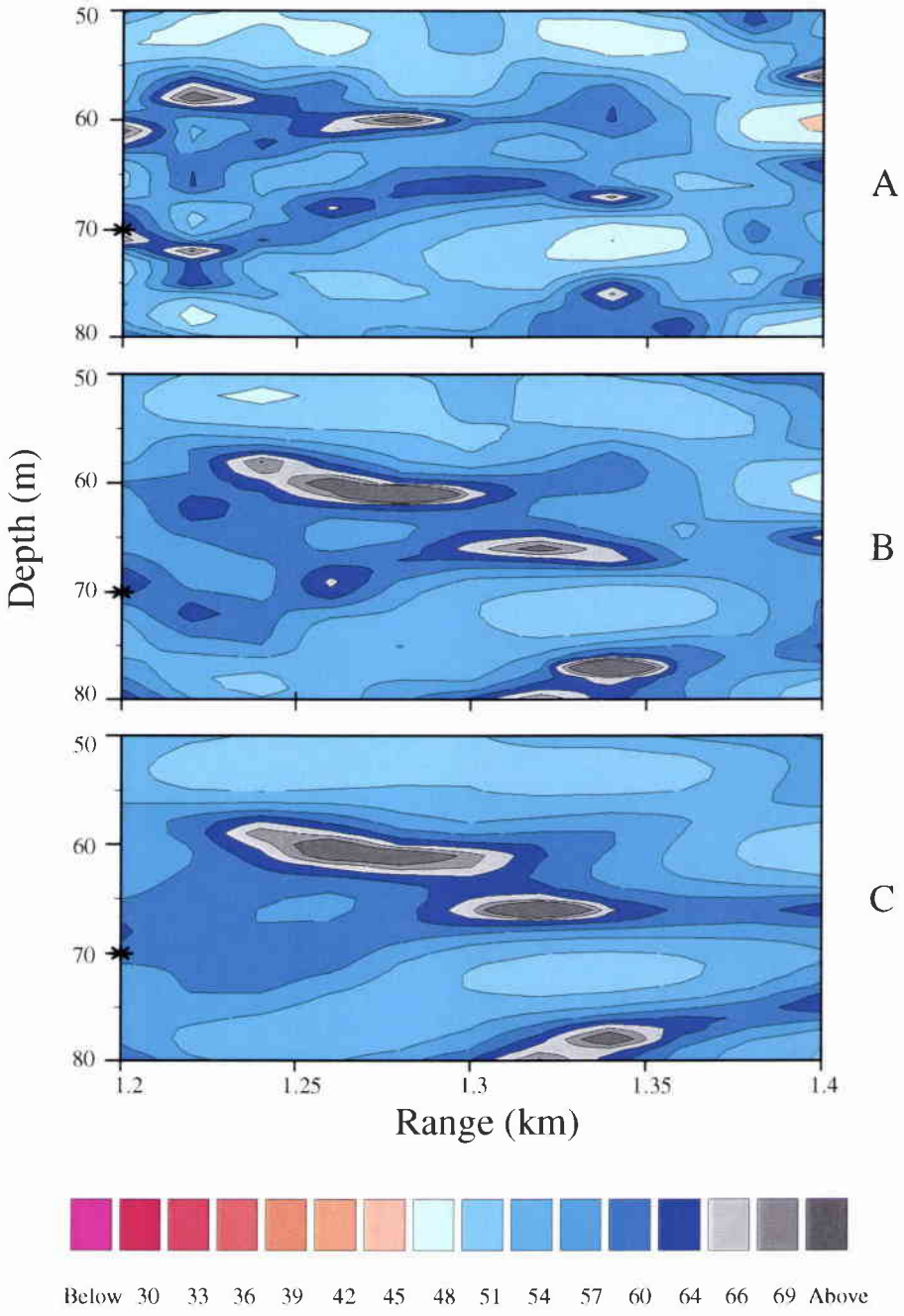

Figure 13 *Transmission loss plots for three sediment thickness: A) 1 m, B) 3 m, and C) 10 m. The silt-sand interface has been used. The source depth is 70 m, and the frequency is 575 Hz.*

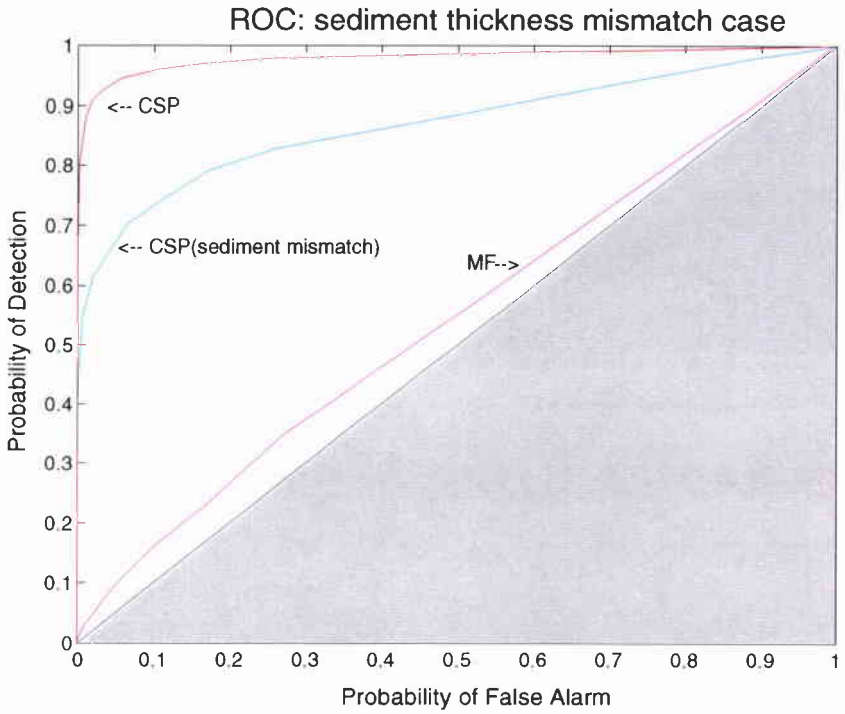

Figure 14 *ROC plots for performance comparison between the matched case CSP, the sediment thickness mismatched case CSP, and the MF processor.*

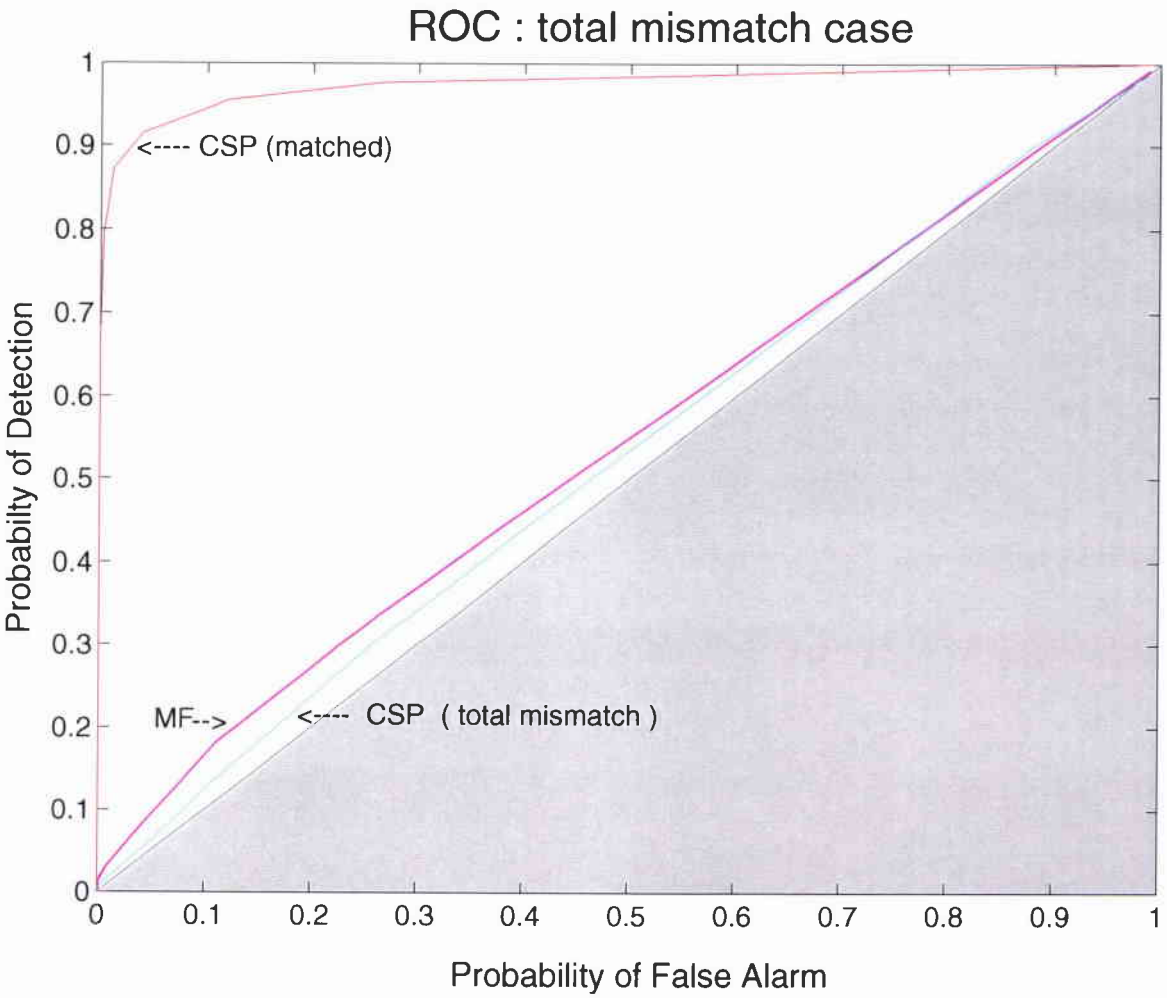

Figure 15 *ROC plots for performance comparison between the matched case CSP, the total (all parameters) mismatched case CSP, and the MF processor.*

5
Global optimization

Global optimization methods have attracted significant attention because they are suitable for locating a global extremum conceled by local extrema in a high dimensional space. The space over which these methods are applied is derived from discretizing a N-dimensional space with N continuously variable parameters. Typically, the outcome is a large configuration space, with a factorially large number of elements that cannot be explored exhaustively. Mainly two such methods, and their variations, are successfully applied to underwater acoustics problems: a) genetic algorithms (GA) [18], [19], [20] which areanalogous to the process of biological evolution and b) simulated annealing (SA) [21] which imitates the cooling process of liquids or metals according to the laws of thermodynamics. In the present study, the SA method is used. Results from a new variation of the SA, named the MUltilayer Simulated Annealing (MUSA), are presented. It will be demonstrated that by coupling these global search methods with the detection algorithm, the performance of the CSP has been significantly improved.

5.1 Simulated Annealing (SA)

In order to introduce the SA scheme, but most importantly to explain its modified version, MUSA, it is necessary to outline how simulated annealing works. The method of SA [22] is an analogy with the process of freezing and crystallization of liquids, or the cooling and annealing of metals. The mobility of molecules at high temperatures is lost when the temperature decreases. When the cooling process is slow, the atoms assume the form of pure crystal which is the minimum energy state of the material. On the other hand, when liquids are cooled quickly they assume an amorphous, polycrystalline state of higher energy. The probability that a system in termal equilibrium at temperature T has energy E is given by the Boltzmann probability distribution

$$P(E) = \exp(-E/kT) \tag{14}$$

where k is Boltzmann's constant which relates temperature to energy. So, even at low temperatures the system might be at a high energy state. The method of SA

utilizes nature's own minimization principle: the search for the global minimum should not be rapid and monotonical to the closest minima. Instead, it should have the freedom, with a small probability, to escape from local minima and look for the absolute minimum solution.

SA is applied to the detection/localization problem in the following way:

1) Search space discretization: the five parameters which comprise the search space, i.e. SSP, sediment-bottom interface, sediment thickness, source range, and source depth. The total number of combinations is 5292. Each combination corresponds to a unique transfer function of the acoustic channel.

2) The "observed" field is simulated using a single set of parameters.

3) Replica fields are generated based on combinations of randomly selected parameters.

4) The CSP filter is applied to compare the observed data with the simulated data. The present set of parameters is preferred to the previous set with the Boltzmann probability $P(\Delta E) = \exp(-\Delta E/kT)$, where ΔE is the CSP output difference for the two parameter sets.

5) The "temperature" T drops by a constant factor after each iteration step which increases the CSP ouput.

6) The process continues until a predefined number of iterations (or temperature level) is reached.

Figure 16 showns the ratio (in dB) of the CSP and the MF output for the entire search space, i.e. for every possible combination of the parameters under investigation. The x-axis corresponds to all combinations of the geometric parameters (range, depth), and the y-axis corresponds to all combinit ons of the environmental parameters (SSP, sediment-subbottom interface, sediment thickness). The maximum output ratio is observed at the point that corresponds to the parameter set which generated the "actual" data. The ROC curves for the optimized CSP algorithm are shown in Fig. 17.

5.2 MUlti-layer Simulated Annealing (MUSA)

SA is a simple yet very efficacious method. This section introduces a modification designated MUlti-layer Simulated Annealing (MUSA). MUSA is designed to overcome the following problem associated with the classical method: At the early stages of the annealing process, the processor has more degrees of freedom to escape from

a region which contains local minima. This ability to hop from one miminum-value zone to another is constrained as the temperature decreases according to the Boltzmann's probability distribution. In cases where there are many local mimina, it may happen that although the search path passes through the area of the global minimum early in the process, it continues examining other possible minima locations at parts of the search space. As time progresses, the "temperature" drops and the freedom to continue changing search areas becomes smaller and the probability that the algorithm remains trapped in a local minima value increases significantly.

This disadvantage of SA is overcome by MUSA in the following way: The new scheme keeps a record of the results of the annealing process. When the "temperature" drops (around one-third of the iteration steps) a second annealing process begins parallel to the first one. The baseline (initial) values and the temperature for the second process are the values which provide the best output, up to that point, in the first process. Then, the two SA algorithms are running simultaneously using different random number generators and different initialization values. At the expense of computation time, this procedure could continue until a large number of SA processes run in parallel. For the present study a 3-layer MUSA was the more sensible configuration because it provided optimum combination of accuracy and time efficiency.

Initial results indicate that the MUSA algorithm demonstrates the following advantages over the conventional SA algorithm:

a) In problematic cases where the search of the initial process diverges from the global minimum, the second process will give the algorithm the opportunity to backtrack in the correct direction.

b) In the case where the initial process converges toward the global minimum, the second, and all subsequent processes in MUSA, will also move in the same direction, only using a different (random) path. At the end, the user can select the best overall solution.

The detection results are shown in Fig. 17. It is shown that for almost the same running time, MUSA clearly outperforms SA. Figure 18 shows the running time for both SA and MUSA compared to the exhaustive search running time.

5.3 Discussion

By utilizing global search methods (both SA and MUSA), the CSP processor overcomes the channel uncertaintly and provides detection performance better than the classical MF method.

Other examples of global optimization algorithms that could have been employed

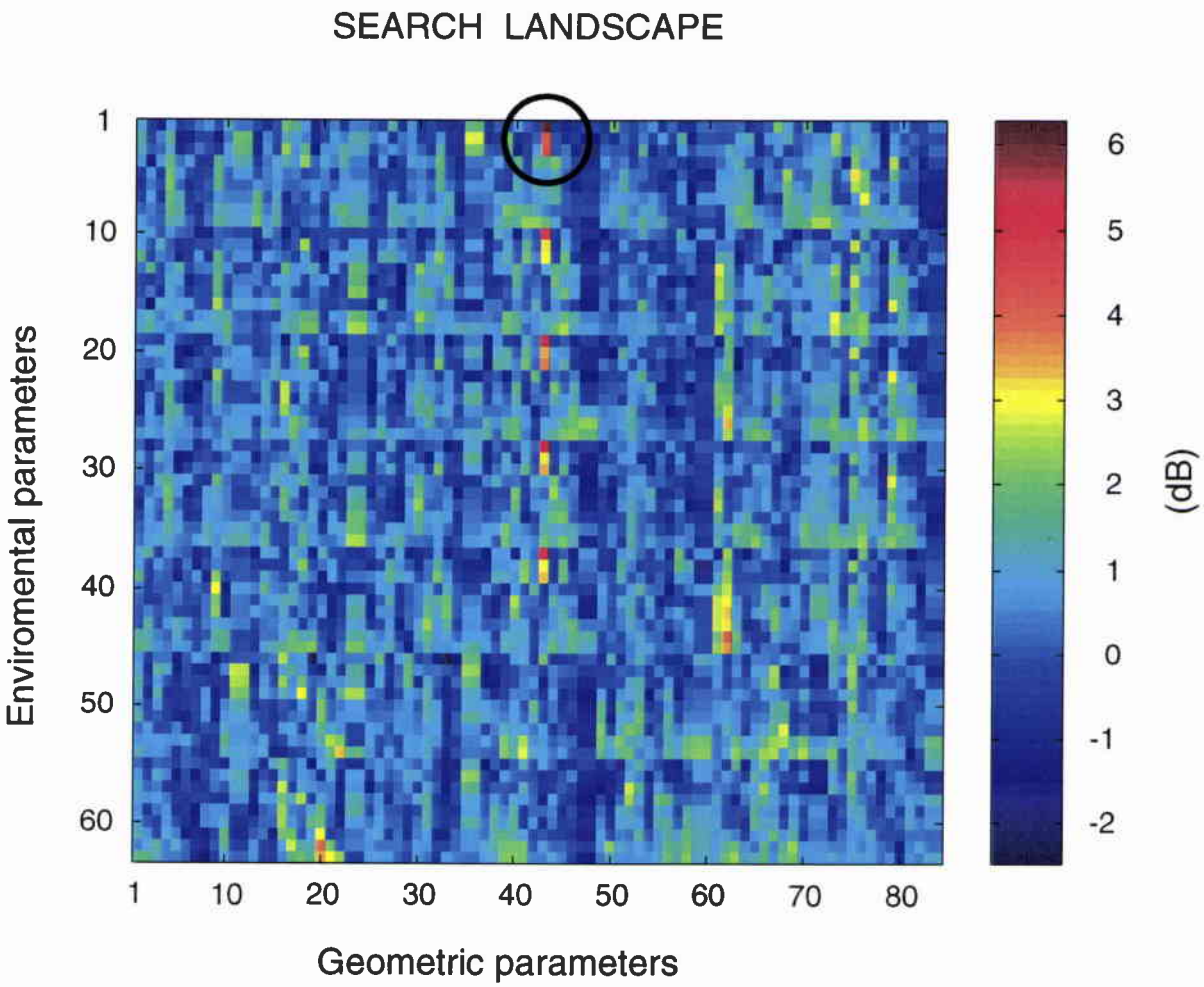

Figure 16 *The output ratio of the CSP and the MF processor for the entire multi-dimensional search space. The vertical axis corresponds to environmental parameters and the horizontal axis to the geometric parameters. The circle indicates the maximum value which corresponds to the correct parameter combination.*

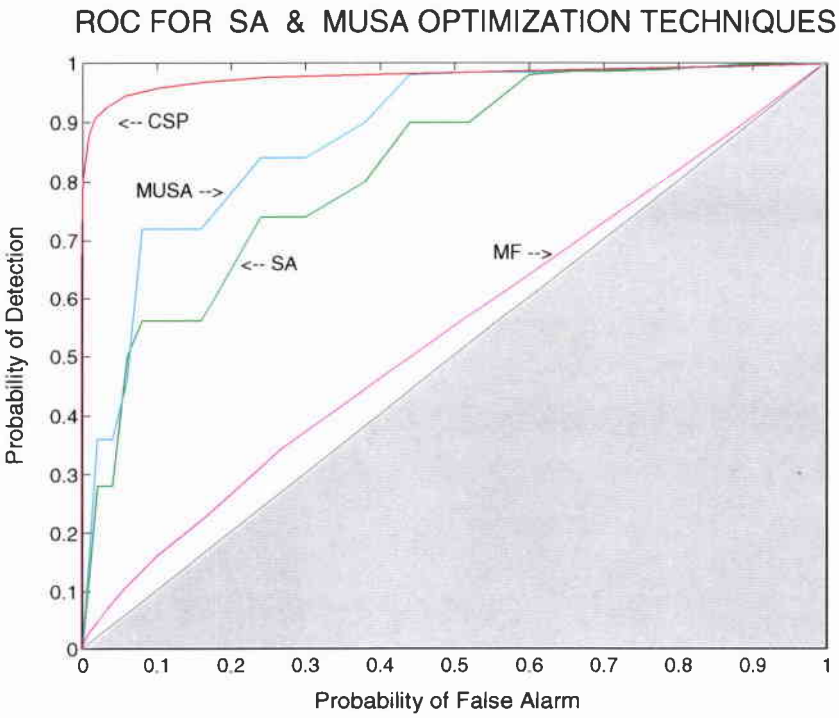

Figure 17 *ROC curves for performance comparison between the matched case CSP, the SA (CSP) case, the MUSA (CSP) case and the MF processor.*

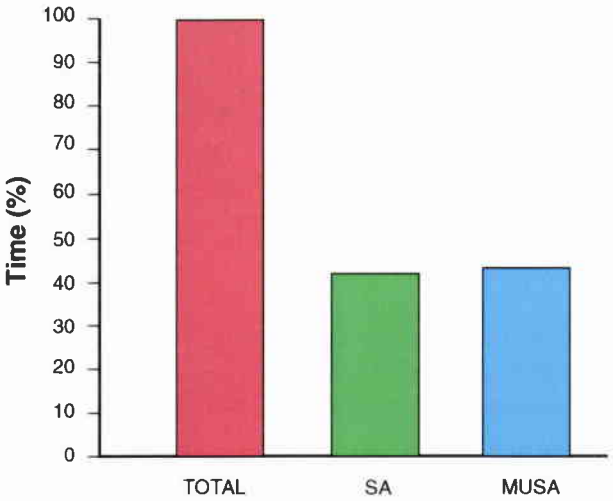

Figure 18 *Computational time comparison of the SA and the MUSA algorithms with the exhaustive search time.*

are the very fast simulated reannealing [23], and the genetic algorithms [18]. All these algorithms have been shown to improve the performance of frequency domain detection/localization processors (e.g. Bartlett processor). The results in this section suggest that these algorithms can be used equally well in MF time domain processing.

6

Conclusions

For a well-defined acoustic channel, the CSP matched filter detector offers the optimum detection performance. For known propagation conditions, the CSP sets the upper limit of matched filter detection performance. However this performance degrades significantly due to propagation condition mismatch. It has been demonstrated that this performance deteriorates significantly on the *a priori* knowledge of propagation channel paramaters. For the particular shallow water channel, and the transmitted LFM pulse (475-675 Hz), the processor is proved to be more sensitive to geometric parameters (coordinates of the source or target) than to environmental parameters (SSP, sediment-subbottom interface, sediment thickness). Under severe channel mismatch condition, the performance of the CSP degrades below the classical MF detection level. However, the employment of global search methods, at the expense of processing time, has been shown to overcome the channel uncertainty and to considerably improve the processor performance. In conjunction with the CSP, two simulated annealing algorithms have been used: SA, the classical metropolis algorithm, and MUSA, a new multi-layered configuration of SA. For the same running time, MUSA proved to give better probability of detection compared to SA. Further work is required to improve the time efficiency of these algorithms. This can be accomplished by employing faster propagation models (ray tracing instead of normal mode codes) and by reducing the dimensions of the search space by identifying correlation patterns between parameters.

References

[1] F.V. Bunkin, I.V. Gindler, A.R. Kozel'skii, Yu.A. Kravtsov, and V.G. Petnikov, Dispersion distortions of complex acoustic signals in shallow ocean waveguides, *Soviet Physics Acoustics*, **35**, No. 5, 461-464, 1989.

[2] M. Wazenski, and D. Alexandrou, Active, wideband, detection and localization in an uncertain multipath environment, *Journal of the Acoustical Society of America*, **101** (4), 1961–1970 (1997).

[3] J.P. Hermand and W.I. Roderick, Acoustic model-based matched filter processing for fading time-dispersive ocean channels: Theory and experiment, *IEEE Journal of Oceanic Engineering*, **18**, No. 4, 447-465, 1993.

[4] D. Alexandrou and G. Haralabus, Channel-sensitive processor: development and detection performance evaluation, *SACLANTCEN*, SR–263, 1997.

[5] F.B. Jensen and M.C. Ferla, SNAP: The Saclantcen Normal-Mode Acoustic Propagation Model, *SACLANTCEN*, SM–121, 1979.

[6] MATLAB User's guide *High-performance numeric computation and visualization software*, The Mathworks Inc, 1993.

[7] F.G. Sremler, *Introduction to communication systems*, Addison-Wesley Publishing Company, 1990.

[8] A.V. Oppenheim and R.W. Schafer, *Digital signal Processing*, Prentice Hall, 1975.

[9] J. V. DiFranco and W. L. Rubin, *Radar Detection*, Artech House Inc., 1980.

[10] R.D. McDonough and A.D. Whalen, *Detection of signals in noise*, Academic Press, 1995.

[11] W.S. Burdic, *Underwater acoustic system analysis*, Prentice Hall Signal Processing Series, 1991.

[12] G. Haralabus, V. Premus, D. Alexandrou, L. W. Nolte, and A. M. Richardson, Source localization in an uncertain acoustic scattering environment, *Journal of the Acoustical Society of America*, **94**, 3379-3386 (1993).

[13] E. L. Hamilton, Geoacoustic modeling of the sea floor, *Journal of the Acoustical Society of America*, **68**, 1313–1340 (1980).

[14] F. B. Jensen, W. A. Kuperman, M. B. Porter, and H. Schmidt, *Computational Ocean Acoustics*, AIP Series in Modern Acoustics and Signal Processing, 1994.

[15] F. B. Jensen, and W. A. Kuperman, Optimum frequency of propagation in shallow water environments, *Journal of the Acoustical Society of America*, **73**, 813–819 (1983).

[16] E. I. Thorsos, The validity of the Kirchhoff approximation for rough surface scattering using a Gaussian roughness spectrum, *Journal of the Acoustical Society of America*, **83**, 79–92 (1988).

[17] R.J. Urick, *Principles of Underwater Sound for Engineers*, McGraw-Hill Inc., 1967.

[18] P. Gerstoft, Inversion of seismoacoustic data using genetic algorithms and *a posteriori* probability distributions, *Journal of the Acoustical Society of America*, **95**, 770–782 (1994).

[19] G. Haralabus, and P. Gerstoft,Source localization in shallow water using multi-frequency processing of shot data, *SACLANTCEN*, SR–253, 1996.

[20] D.F. Gingras and P. Gerstoft, " Inversion for geometric and geoacoustic parameters in shallow: Experimental results", *Journal of the Acoustical Society of America*, **97**, 3589–3598 (1995).

[21] M. D. Collins, W. A. Kuperman, and H. Schmidt, " Nonlinear inversion for ocean-bottom properties ", *Journal of the Acoustical Society of America*, **92**, 2770–2783 (1992).

[22] W. H. Press, S. A. Teukolsky, W. T. Vettering, and B. P. Flannery, *Numerical Recipes in C*, Cambridge University Press, 1992.

[23] L. Ingber, " Very fast simulated re-annealing", Mathl Computational Modelling, No. 8, 967–973 (1989).

Report no. changed (Mar 2006): SR-275-UU

Document Data Sheet

Security Classification		Project No.
NATO UNCLASSIFIED		041-2
Document Serial No.	**Date of Issue**	**Total Pages**
SR-275	October 1997	38 pp.

Author(s)

Haralabus, G.

Title

Channel sensitive processor: sensitivity and optimization study

Abstract

The detection performance of the Channel-Sensitive Processor (CSP) has been tested in dense multi-path conditions. It was demonstrated that, for a known propagation channel, the CSP outperforms the conventional matched filter technique. However, in an uncertain environment, the probability of detection decreases according to the degree of mismatch between the assumed and the actual channel characteristics. It was found that the processor is more sensitive to geometric parameters (source range and depth) than to environmental parameters (sound velocity profile, sediment-subbottom interface, sediment thickness). To overcome the performance degradation due to channel mismatch, the CSP method was utilized in conjunction with two global optimization algorithms: the classical simulated annealing (SA) and a multi-layer simulated annealing (MUSA) method. At the expense of processing time, it has been found that the optimization methods reduce the channel mismatch effect and improve considerably the detection performance of the CSP.

Keywords

Matched Filter (MF) – Channel-Sensitive Processor (CSP) – sensitivity study – global optimixation – Simulated Annealing (SA) – Multi-layer Simulated Annealing (MUSA)

Issuing Organization

North Atlantic Treaty Organization
SACLANT Undersea Research Centre
Viale San Bartolomeo 400, 19138 La Spezia, Italy

[From N. America: SACLANTCEN (New York) APO AE 09613]

Tel: +39 (0)187 540 111
Fax:+39 (0)187 524 600

E-mail: library@saclantc.nato.int

Initial Distribution for SR 275

Ministries of Defence

DND Canada	10
CHOD Denmark	8
DGA France	8
MOD Germany	15
HNDGS Greece	12
MARISTAT Italy	9
MOD (Navy) Netherlands	12
NDRE Norway	10
MOD Portugal	5
MDN Spain	2
TDKK and DNHO Turkey	5
MOD UK	20
ONR USA	42

NATO Commands and Agencies

NAMILCOM	2
SACLANT	3
CINCEASTLANT/ COMNAVNORTHWEST	1
CINCIBERLANT	1
CINCWESTLANT	1
COMASWSTRIKFOR	1
COMMAIREASTLANT	1
COMSTRIKFLTANT	1
COMSUBACLANT	1
SACLANTREPEUR	1
SACEUR	2
CINCNORTHWEST	1
CINCSOUTH	1
COMEDCENT	1
COMMARAIRMED	1
COMNAVSOUTH	1
COMSTRIKFORSOUTH	1
COMSUBMED	1
NC3A	1
PAT	1

Scientific Committee of National Representatives

SCNR Belgium	1
SCNR Canada	1
SCNR Denmark	1
SCNR Germany	1
SCNR Greece	1
SCNR Italy	1
SCNR Netherlands	2
SCNR Norway	1
SCNR Portugal	1
SCNR Spain	1
SCNR Turkey	1
SCNR UK	1
SCNR USA	2
French Delegate	1
SECGEN Rep. SCNR	1
NAMILCOM Rep. SCNR	1

National Liaison Officers

NLO Canada	1
NLO Denmark	1
NLO Germany	1
NLO Italy	1
NLO Netherlands	1
NLO Spain	1
NLO UK	1
NLO USA	1

Sub-total	208
SACLANTCEN	30
Total	238